Hindawi
Geofluids
Volume 2023, Article ID 9740015, 12 pages
https://doi.org/10.1155/2023/9740015

Research Article

Experimental Study on the Distribution of Retained Fracturing Fluids and Its Effect on the Permeability and Wettability in Tight Oil Reservoirs

Tuan Gu,[1] **Zhilin Tuo**,[2] **Tao Fan**,[1] **Dongpo Shi**,[1] **Chun Mu**,[1] **Shucan Xu**,[3] **and Desheng Zhou**[3]

[1]*Research Institute of Petroleum Exploration and Development, Liaohe Oilfield Company of Petro, China*
[2]*Gas Recovery Plant No.2, PetroChina Changqing Oilfield Company, China*
[3]*College of Petroleum Engineering, Xi'an Shiyou University, China*

Correspondence should be addressed to Desheng Zhou; x13689261423@163.com

Received 14 November 2022; Revised 25 November 2022; Accepted 21 March 2023; Published 24 April 2023

Academic Editor: Daoyi Zhu

It is not clear how the distribution of retained fracturing fluids and its effect on the permeability and wettability in tight oil reservoirs interact. Especially, there are more qualitative studies and less quantitative studies on this issue. Under laboratory experimental conditions, this paper clarifies the distribution of retained fracturing fluids in the core and reveals the influence rule of retained fracturing fluids on tight reservoir permeability and wettability. It is found that the main retention space of retained fracturing fluids in a tight reservoir is a microporous interval, and the residual oil after oil displacement by retained fracturing fluids mainly exists in the core in the form of dots or porphyries. The smaller permeability and porosity of the core will lead to more retained fracturing fluids. The permeability of different cores after fracturing fluid retention has decreased to varying degrees compared with that before fracturing fluid retention. The wettability of core slices before and after fracturing fluid retention was tested, and the effect of retained fracturing fluids on reservoir wettability was not significant. This study has important significance for improving the recovery of tight oil reservoirs and enhancing the understanding of postfracturing fluid retention.

1. Introduction

The tight oil is widely distributed and has huge reserves in China and will gradually become the main force in the supply of oil and gas resources [1]. However, the compaction of a tight oil reservoir is strong in the diagenesis [2]. Because the rock is dense and the particles are small, the porosity and permeability of the reservoir are low and the physical properties are relatively poor, which brings a series of problems to the development of a tight oil reservoir [3]. The combination technology of hydraulic fracturing and long horizontal well is the most effective method to develop a tight oil reservoir at present [4].

During the fracturing, a large amount of fracturing fluids are injected into the formation, and the flow-back rate is usually low [5]. A large amount of fracturing fluids is retained in the formation, and previous researches on fracturing fluid retention in the formation have been conducted. Williams [6] divided the retention process of fracturing fluids into three stages: nonformation of filter cake, formation of filter cake, and dynamic filtration. Yew et al. [7] considered the influence of natural fractures existing in low permeability reservoirs on fracturing fluid retention based on the research of Economides. Rodgerson [8] studied and analyzed the fracturing fluid retention state of the reservoir when there are natural fractures. However, due to its complex conditions, this study did not obtain an effective retention model for natural fracture reservoirs. Outmans [9] proposed a model including the relationship between porosity, compressibility and pressure, and permeability to predict

dynamic filtration. It is found that the dynamic filtration rate is independent of the shear rate when the mud dynamic filtration reaches equilibrium. Vinod et al. [10] calculated that the microparticles in the fluids will block the rock pores, block the fluid flow, and cause damage to the formation to some extent. It is concluded that the effective permeability of the formation is related to the polymer, and the polymer will cause additional pressure difference to the fracturing fluid filtration. Mathias and Van Reeuwijk [11] proposed one-dimensional and two-dimensional fracturing fluid filtration calculation models. The calculation results are far from the actual filtration situation, and the simulation effect is poor. For tight reservoirs, the fracturing fluid retention has a serious impact on the physical properties of the reservoir. At present, the research on the fracturing fluid retention is mainly focused on establishing the mathematical model of the retention and correcting the model, but the method of the impact of the retention on the physical properties of rocks by means of indoor core experiments has not been adopted [12, 13].

Two important parameters related to the physical properties of tight reservoir rocks include permeability and wettability [14]. In 1964, Pirson et al. [15] proposed a model for calculating relative permeability from resistivity, tested their model through experimental data, and adjusted the model under different conditions with different correction coefficients. For example, the gas-water model is different from the oil-water model. Through the optimization of permeability modeling, accurate permeability parameters are obtained. The prediction methods for permeability are mainly divided into two categories: one is statistical modeling based on core analysis data, and the other is the learning modeling method using data mining. Akande et al. [16] established a permeability prediction model based on the random selection of particle swarm optimization algorithm, combined with support vector function to simplify the regression problem, and improved the generalization ability and prediction accuracy of the model. Purcell [17] established the Purcell model applicable to sandstone reservoir; Thomeer [18, 19] established the Thomeer model applicable to sandstone reservoir; Kolodzie [20] divided the petrophysical category of sandstone reservoir and carbonate reservoir with the corresponding pore throat radius when the mercury inflow saturation is 35% and established the Winland-r35 model. Since then, other scholars such as Rezaee et al. [21] have studied tight sandstone gas reservoirs in Western Australia and found that the correlation between the corresponding pore throat radius and permeability is the highest when the mercury inflow saturation is 10%; Min et al. [22] believed that when the stress is small, the permeability of broken rock decreases with the increase of stress amplitude, while when the stress ratio is large enough, the permeability increases with the increase of stress. Larsen et al. [23] pointed out that the geological tectonic field has a great impact on the permeability of carbonate rocks, and the tensile stress caused by fracture is helpful to increase the permeability of carbonate rocks. In fact, a large amount of retained filtration fracturing fluids can change the state of tight reservoir rocks, such as the generation of new microfractures, which will lead to significant changes in permeability. There are more qualitative studies than quantitative studies on this issue.

Rock wettability is one of the important characteristics of rock physics [24]. The nuclear magnetic resonance T2 spectrum is commonly used to reflect the pore size distribution of hydrophilic rocks, but when the rock wettability changes, the nuclear magnetic resonance response based on the position of fluid relative to the rock pore surface will change [25, 26]. Howard [27] was the first to attempt to evaluate the wettability of reservoir rocks by quantitative means and to establish a relationship between the relaxation movement of saturated water and water saturation and wettability. Straley et al. [28] introduced the wetting parameters and oil saturation into the surface relaxation formula and established the relationship between the relaxation time and the surface relaxation rate, specific surface area, oil saturation, and wetting parameters. In 2003, Fleury and Deflandre [29] proposed an NMR wettability index that is more consistent with the physical properties of rocks; however, this method requires complete separation of T2 relaxation of oil and water. Guan et al. [30] proposed to quantitatively indicate the wettability characteristics of reservoir rocks by using the change of the arithmetic mean value of nuclear magnetic relaxation time before and after oil flooding and water flooding. The calculation result of this method is different from the value range of the Amott index, so it is impossible to directly make a numerical comparison. Al-Mahrooqi et al. [31] published an article on the evaluation of rock wettability in 2006 by combining nuclear magnetic resonance experiments and numerical simulation. By establishing a capillary bundle seepage model of triangular interface considering liquid-solid interaction, the expression of nuclear magnetic resonance T2 spectrum under different displacement pressures (i.e. different microdistribution of oil and water) was derived, and the influence of different wettability on nuclear magnetic resonance response was quantitatively explained from the rock pore size. Johannesen et al. [32] proposed to calculate the difference between the relaxation time corresponding to the peak value of the right peak of T2 relaxation spectrum of saturated oil state in other wettability states of cores and the standard based on the relaxation time corresponding to the peak value of the right peak of T2 relaxation spectrum of saturated oil state in strong hydrophilic cores as the evaluation parameter of rock wettability. Chen et al. [33] found that the change of the effective surface relaxation rate of oil or water in saturated uncompacted silica sand or calcite porous media was in good agreement with the wetting size measured by the contact angle and proposed to establish the nuclear magnetic resonance wetting index by obtaining the effective surface relaxation rate from the T2 surface relaxation term. Minh et al. [34] proposed a study on rock wettability based on restricted diffusion, which can be applied to downhole measurement. Rabiei et al. [35] studied the thickness of the water film on the sandstone wall when water and oil exist at the same time and believed that after the water film was stripped, the crude oil directly contacted the sandstone surface, so the sandstone surface showed part of the oil wet, while other parts were still wet. Pratten and

Craig [36] believed that neutral wettability existed in most reservoirs, which are neither lipophilic nor hydrophilic, and there is no strong selectivity for both. Gachot et al. [37] pointed out that the rock surface with strong hydrophilicity will change to weak hydrophilicity after contacting with crude oil, and the small pores in the core are mostly water wet, while the water wetness of large pores is relatively weak. Therefore, it is necessary to test the influence of fracturing fluid retention on reservoir wettability through a more reasonable experimental design and method.

Under laboratory experimental conditions, this paper studies the influence of retained fracturing fluids on reservoir physical properties by using core thin section and nuclear magnetic resonance technology, clarifies the distribution rule of retained fracturing fluids in core, and reveals the influence rule of retained fracturing fluids on tight reservoir permeability and wettability. This study has important reference significance for improving the recovery of tight oil reservoirs and enhancing the understanding of postfracturing fluid retention.

2. Materials and Methods

2.1. Experimental Materials. The materials used in this study include rock slices and rock column samples, which are, respectively, used to carry out thin section observation experiments and permeability evolution experiments. The basic parameters of the slices used are shown in Table 1. The diameter is about 2.5 cm, the thickness is 1 mm to 3 mm, and the permeability is generally low. As shown in Table 2, the column samples are more than 4 cm in length, less than 10% in porosity, and higher in permeability. In addition, the experimental materials also include simulated retained fracturing fluids, kerosene, $MnCl_2$ solution, and other liquid materials.

2.2. Experimental Method. In order to study the oil-water distribution in tight oil reservoirs after fracturing, nuclear magnetic equipment is used for monitoring [38]. The instrument used in the experiment is MesoMR23-60H-I low-field NMR analyzer, and the manufacturer is Suzhou Niumag Analytical Instrument Corporation. The magnet type is a permanent magnet. The magnetic field intensity is 0.5 ± 0.05 T. The probe coil is 25 mm. The magnet temperature is 32°C. The dominant frequency of the instrument is 23 MHz. The sample size should be 25 mm in diameter and about 50 mm in length. The ambient temperature is 15-25°C, and the relative humidity is 50-70%, as shown in Figure 1. Laboratory experiments were carried out on the tight sandstone core of Chang 7 Member of Yanchang Formation in Ordos Basin, using nuclear magnetic resonance technology, scanning electron microscopy, casting thin section and mirror observation photography, and other technical means.

In order to prevent the influence of hydrogen signal in distilled water on the oil signal in the core, the experimental liquid is a manganese chloride solution with a mass fraction of 40%. This is because after the divalent manganese ions fully diffuse into the core pores, the water signal will be shielded, and manganese chloride is not soluble in oil, so the oil signal will not be affected [39]. In this way, the water and oil signals will be separated to facilitate T2 spectrum observation. The experimental process and equipment are shown in Figure 2. The main test steps are as follows: (1) use the wire cutter to cut the core into thin slices (1-2 mm thickness) of the required size and put the core into a 70°C thermostat until the dry weight of the slices does not change. Measure the diameter, thickness, quality, permeability, and other basic parameters of the thin film and photograph the dry thin film samples in full view and local view with a stereoscopic microscope. (2) Pressurize and saturate the dried core slice to simulate formation water condition for 24 h to obtain the core slice saturated with water. Scan and image the saturated core slice by nuclear magnetic resonance to obtain the T2 spectrum and imaging image of saturated water. Dry the scanned core in a constant temperature oven at 70°C, and then saturate the core slice in the configured 40% manganese chloride solution. (3) Put the core slice

Table 1: List of core slice parameters.

No.	Diameter/mm	Thickness/mm	Weight/g	Permeability/mD
A-1	25.37	2.57	2.295	0.024
A-2	25.33	1.97	1.887	0.091
A-3	25.33	2.53	2.664	0.034
A-4	25.34	2.18	2.247	0.088
A-5	25.33	2.11	2.148	0.034
B-4	25.36	1.81	1.776	0.029

Table 2: Basic parameters of the experimental core.

No.	Length (cm)	Diameter (cm)	Weight (g)	Porosity (%)	Permeability (mD)
E-1	4.486	2.517	59.144	7.21	0.564
E-2	4.064	2.525	51.726	6.35	0.535
E-3	4.128	2.536	53.733	3.97	0.278
E-4	4.825	2.528	62.860	6.85	0.494
E-5	4.503	2.509	55.655	4.67	0.389

Figure 1: Low-field NMR analyzer.

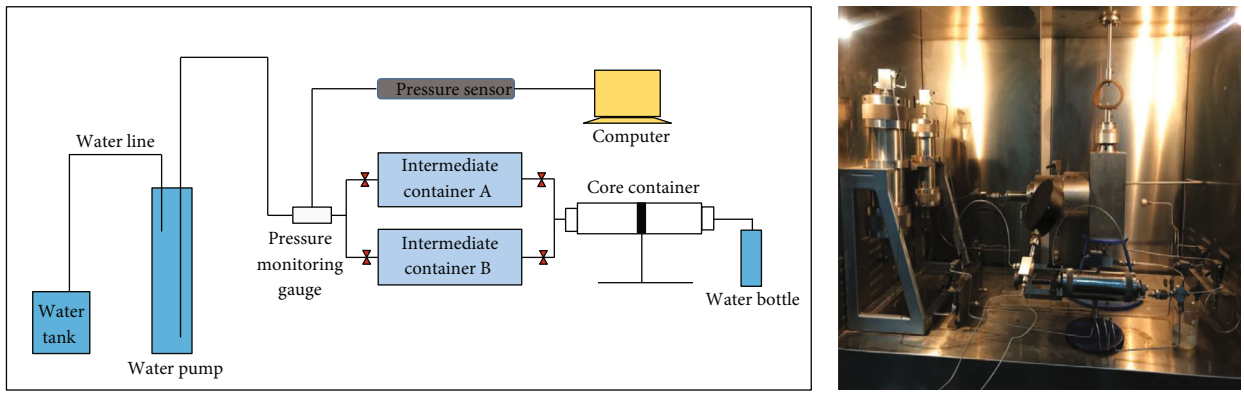

(a) Physical diagram (b) Schematic diagram

Figure 2: Core flow chart.

saturated with 40% manganese chloride solution into the nuclear magnetic resonance analyzer for scanning and imaging and get the T2 spectrum and imaging map of saturated manganese. Then, use the stereoscopic microscope to take pictures in full and local view. Put the core slice after the experiment into the displacement device to start oil flooding to the outlet end without water and create the bound water state of the core. (4) Put the core slice with bound water into the nuclear magnetic resonance analyzer for scanning and imaging, obtain the T2 spectrogram and imaging image, and use the stereoscopic microscope to take pictures in a full field of view and local field of view. (5) Put the original oil-bearing core slices in the irreducible water state into the displacement device and displace them with 40% manganese chloride solution to the outlet end without oil production, scan and image them with the nuclear magnetic resonance analyzer, and take photos with the stereoscopic microscope. (6) Use oil to reverse drive the core slice after water flooding to the outlet without water. Use the MRI analyzer for scanning and imaging, and then use the stereoscopic microscope for taking pictures [40].

In order to study the effect of retained fracturing fluids on the permeability of a tight reservoir, a permeability monitoring experiment after fracturing fluid retention was carried out. The experimental steps are as follows: (1) cut the core into the size required by the experiment, wash the oil, dry the core, and measure its dry weight and size; (2) gas logging core porosity and permeability; (3) pressurize the core to 20 MPa saturated water; (4) displace the saturated kerosene by the core, and weigh its wet weight to calculate the porosity and permeability; (5) put the core into the displacement device to start water drive oil until the outlet end is no longer producing oil. Record the volume of oil expelled V1. At this time, the volume of oil expelled is equal to the volume of water retained in the core. For water drive cores, this process simulates the fracturing fluid retention into the formation during development; (6) oil reversely displaces water until there is no water at the outlet end. Record the volume of water expelled, V2. This process simulates the process of oil entering the wellbore after fracturing. At this time, the water loss in the core should be V1-V2.

In order to analyze the influence of fracturing fluids on reservoir wettability, the cores before and after fracturing fluid retention were treated with saturated water and saturated oil, and nuclear magnetic resonance scanning was performed on them. The NMR data of fracturing fluids before and after fracturing fluid retention are used to analyze the change of core mixing wettability. The specific steps are as follows: (1) wash and dry the compact rock sample slices; (2) test the T2 relaxation time spectrum of NMR after the core is saturated with simulated formation water condition; (3) displace the saturated water core by 40% $MnCl_2$ solution to shield the water phase signal in the core and scan the core again by NMR, reducing the signal to less than 1% of the original signal; (4) put the rock sample in the displacement device, and then conduct oil displacement water experiment until there is no water output at the outlet end, and establish irreducible water saturation; (5) measure the T2 atlas of saturated oil cores in the original formation state and compare the T2 relaxation time atlas in the saturated simulated formation water state with it; (6) repeat the above steps for the core slice after fracturing fluid retention to obtain T2 relaxation time atlas of saturated water and saturated oil after fracturing fluid retention.

3. Experimental Results and Discussion

3.1. Oil-Water Distribution in Tight Oil Reservoirs after Fracturing. Figure 3 shows the pseudocolor NMR images of different stages of core slice A-1. Except for the images of saturated samples, the other images only reflect the strength of oil signals. The signal of the A-1 oil displacement manganese water sample of the core slice is not as strong as that of the saturated water sample, which indicates that manganese water is not completely driven out during oil displacement, and there is still a lot of bound water in the micropores of the core slice. However, the water drive oil sample signal of core slice A-1 decreases again, indicating that a large amount of oil is displaced to the outside by the differential pressure of displacement, and only a small part of the oil remains in the core slice. When it comes to oil reverse displacement, although the signal strength is enhanced, it cannot reach the

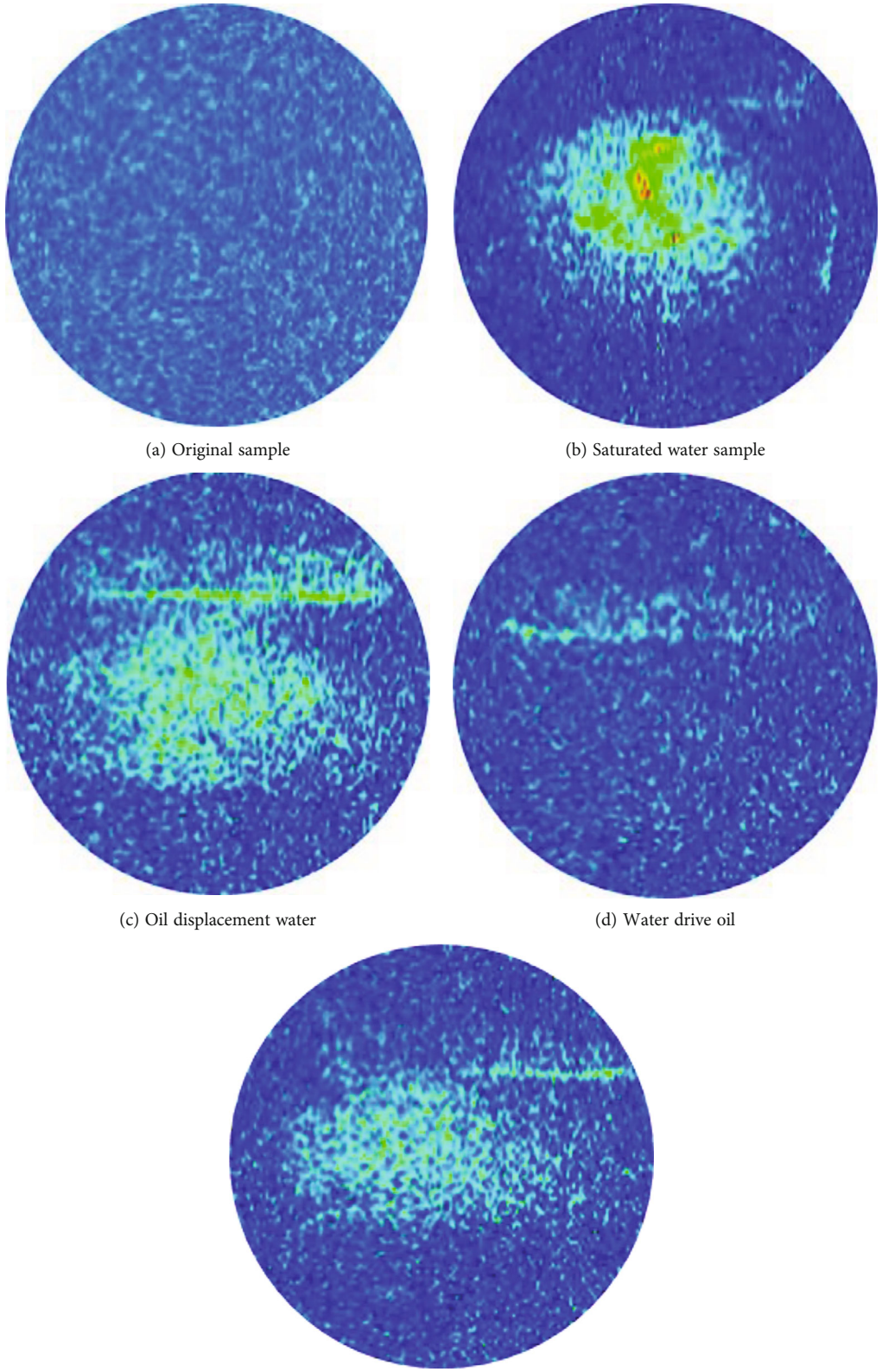

(a) Original sample

(b) Saturated water sample

(c) Oil displacement water

(d) Water drive oil

(e) Oil reverse displacement water

Figure 3: Pseudocolor NMR images of different stages of core slice A-1.

signal strength under the original oil saturation state, indicating that it is difficult for oil to enter the pores filled with fluid again, and most of the oil and water in the macropores can only move along the direction of the pore path with small capillary resistance, which results in a large amount of water remaining in the reservoir due to retention [41].

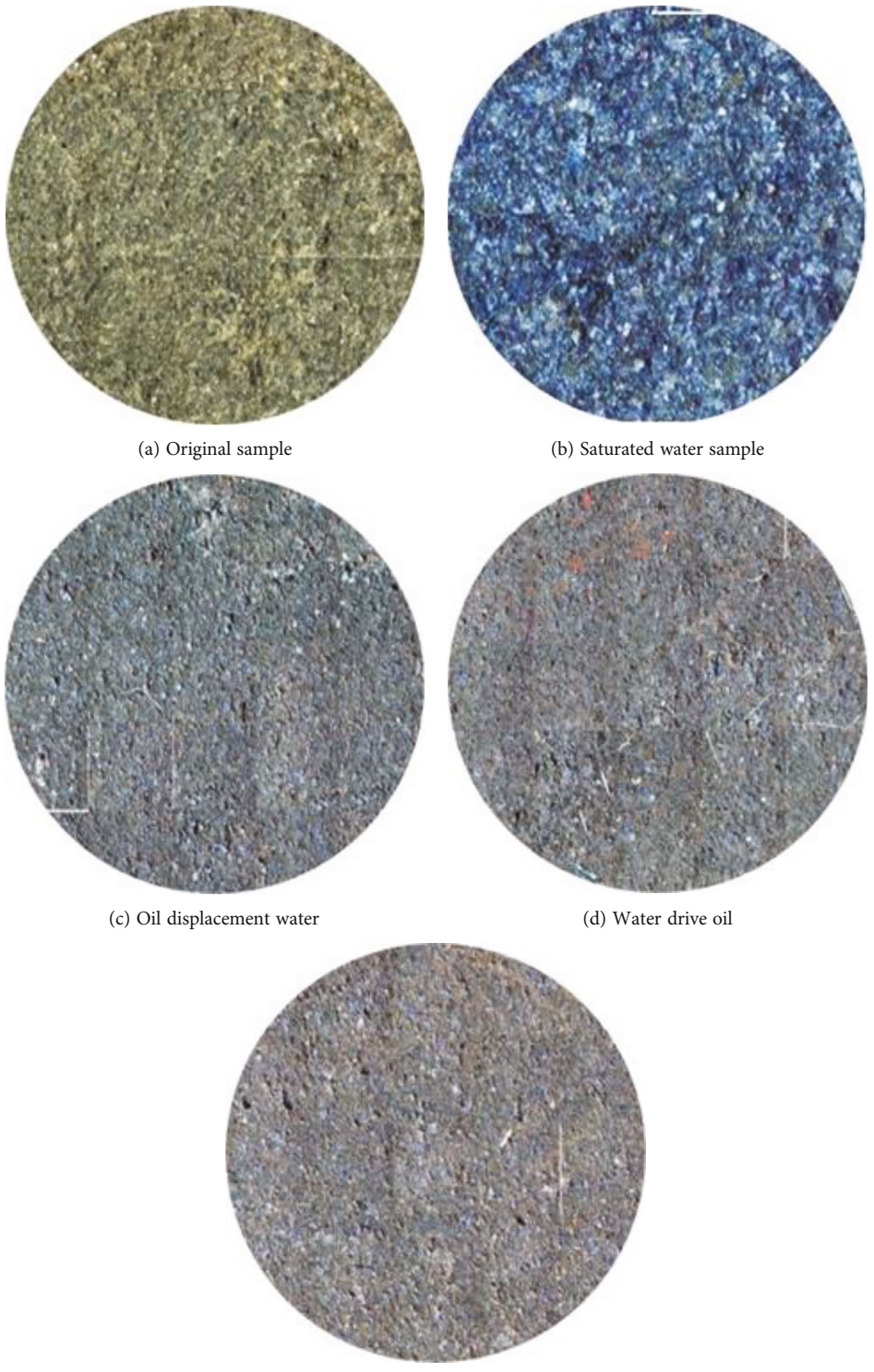

(a) Original sample

(b) Saturated water sample

(c) Oil displacement water

(d) Water drive oil

(e) Oil reverse displacement water

Figure 4: Photographic images for the stereoscopic microscope of different stages of core slice A-1.

The following images which are taken with a stereoscopic microscope can be more intuitive to see the distribution of retained fracturing fluid in the core slice. Figure 4 shows the photographic images for the stereoscopic microscope of different stages of core slice A-1. After oil displaces manganese water, the blue color on the thin slice obviously fades, indicating that a large amount of oil has saturated into the inner part of the slice.

Figure 5 shows the local enlarged view of core slice A-1 after oil displacing manganese water. The position of the black circle in the figure is red kerosene saturated into the inner part of the sheet, but there are still many blue parts

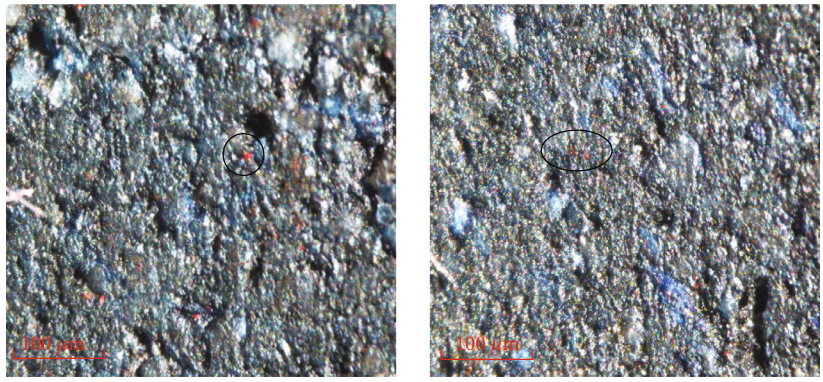

Figure 5: Local enlarged view of core slice A-1 after oil displacing manganese water.

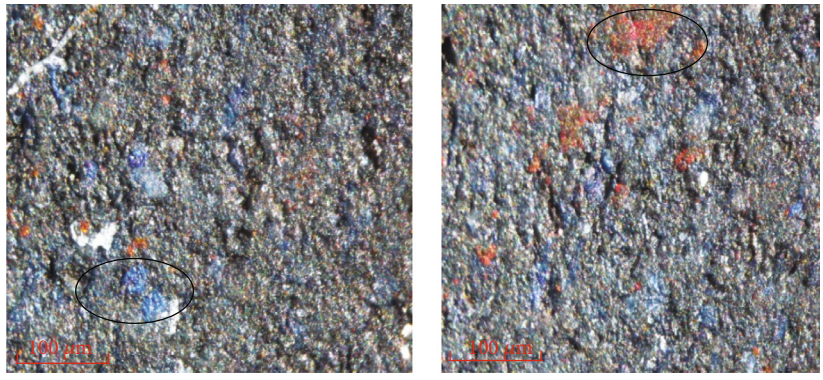

Figure 6: Local enlarged view of core slice A-1 after water flooding.

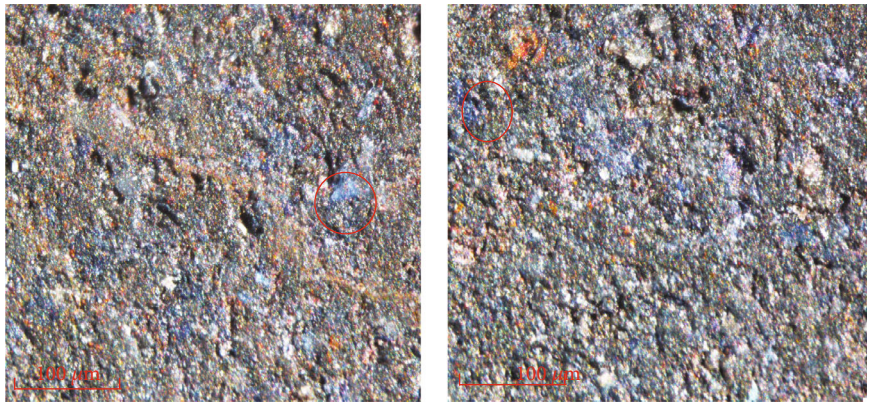

Figure 7: Local enlarged view of core slice A-1 after oil reverse displacement.

in the figure, indicating that there is still a large amount of manganese water in the sheet at this time. The blue parts in the figure are dark and light, indicating the different bound water volumes, which is due to the overlapping of porosity phases in the picture. The three-dimensional distribution of pores in the sheet is very obvious, and there are many small pores developed.

Figure 6 shows the local enlarged view of core slice A-1 after water flooding. The position of the black circle in the figure is the residual oil after water flooding. The residual oil is mainly concentrated in the small and medium-sized pores. In the extremely small pores, because the oil is basically not saturated into the oil when saturated, there is very little residual oil in the too-small pores, and the oil in the large pores is basically expelled by water, so there is less residual oil in the large pores. During displacement, microfingering will occur, that is, the retained fracturing fluids will easily move along the direction of low capillary resistance and high permeability. When multiple projecting water phase channels are closed, there will be a large amount of residual oil in the area between the water channel and the water channel that is not swept by the injected water. A large amount of residual oil mainly exists in the matrix that is not swept by water in the form of spots, and some residual oil

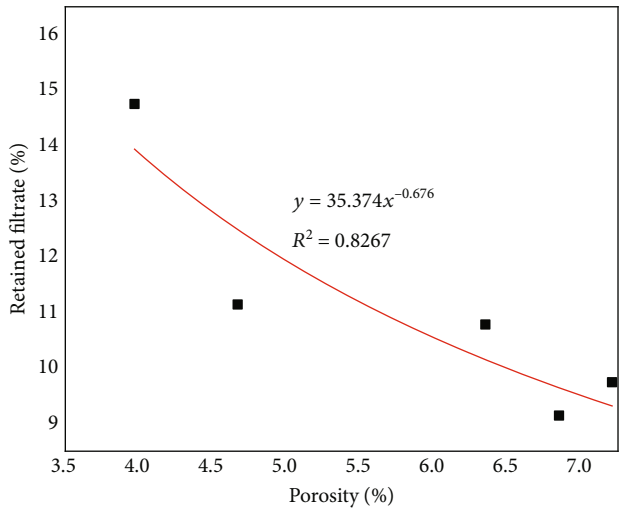

Figure 8: Relationship between fracturing fluid retention and porosity.

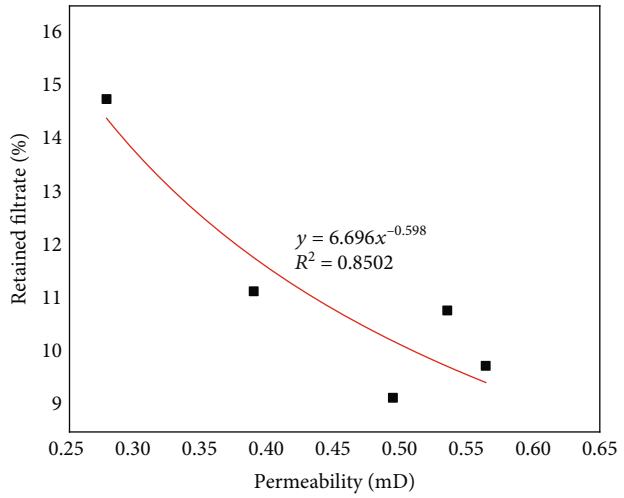

Figure 9: Relationship between fracturing fluid retention and permeability.

exists in the matrix that is easy to flow in the form of mutual infection of oil and water.

Figure 7 shows the local enlarged view of core slice A-1 after oil reverse displacement, and the red circle represents the retained fracturing fluids trapped in the core. It can be seen from the figure that after the oil reverse drive, there is a large amount of kerosene in the core, but the oil reverse drive does not drive out all the retained fracturing fluids in the slice, and some of it remains in the core. For tight reservoirs, as more and more water is retained in the reservoir rocks due to fracturing fluid retention, plus reasonable shut-in time, more oil will be produced due to imbibition displacement, and the production will increase significantly.

3.2. Influence of Fracturing Fluid Loss on Permeability. Through the curve analysis in Figures 8 and 9, it can be concluded that with the increase of porosity, the amount of retained fracturing fluids in the core will decrease, while

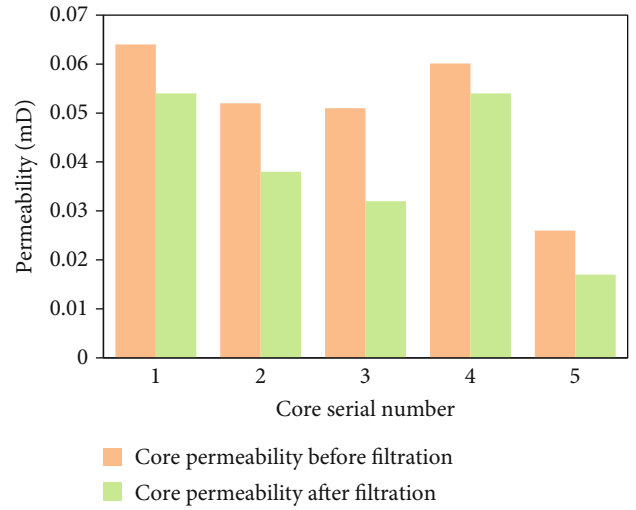

Figure 10: The permeability change before and after core fracturing fluid retention.

when the permeability decreases, the amount of retained fracturing fluids in the core will increase. Among them, compared with porosity, the correlation between core permeability and retained water is good. The results show that, in the actual production process, there will be more fracturing fluid retention in the tight core and more fracturing fluid retention in the reservoir; then, the retained fracturing fluids in the reservoir will replace the oil in the micro pores under the appropriate well shut-in time, thus producing more oil. This is different from the traditional production wells that require rapid flow-back. For conventional oil well exploitation, the reservoir permeability is relatively high, and the retained fracturing fluids that can be retained in the formation itself is less, so the displacement effect is not significant. Therefore, the rapid flow-back method is required to effectively avoid reservoir damage. However, in the tight reservoir, it has low permeability, and the fracturing fluids is mostly slippery water system, so the reservoir itself is less damaged by the fracturing fluids. At the same time, the fracturing fluids flow-back rate is very low. In addition, the retained fracturing fluids will displace the oil that is difficult to flow in the tight reservoir, thus increasing the production of oil wells. Therefore, the most important thing in tight reservoirs is to determine the reasonable shut in time and give full play to its advantages of imbibition displacement, rather than blindly pursuing a high flow-back rate.

Figure 10 shows the permeability change before and after core fracturing fluid retention. It can be seen from the figure that the permeability after fracturing fluid retention has decreased to a certain extent compared with the permeability before core fracturing fluid retention. This is due to the high content of clay minerals in low-permeability reservoirs. In the process of saturated oil, some oil will be adsorbed by clay minerals. With their gradual accumulation and occupation, the originally small pore space will be further reduced, which greatly reduces the porosity and permeability, increases the thickness of the boundary layer, and aggravates the influence of the boundary layer on seepage. The pore space of clay

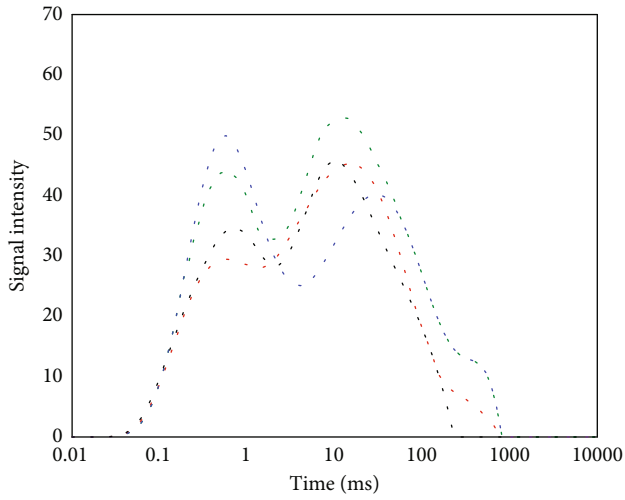

% (saturated water before filtration)
% (saturated oil before filtration)
% (saturated water after filtration)
% (saturated oil after filtration)

(a) Core slice A-1

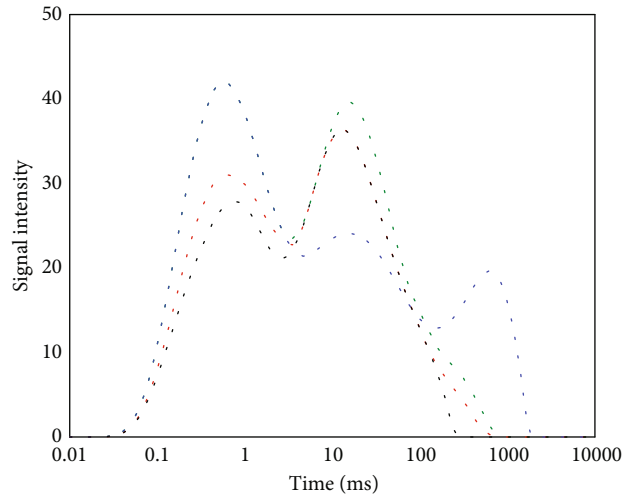

% (saturated water before filtration)
% (saturated oil before filtration)
% (saturated water after filtration)
% (saturated oil after filtration)

(b) Core slice A-2

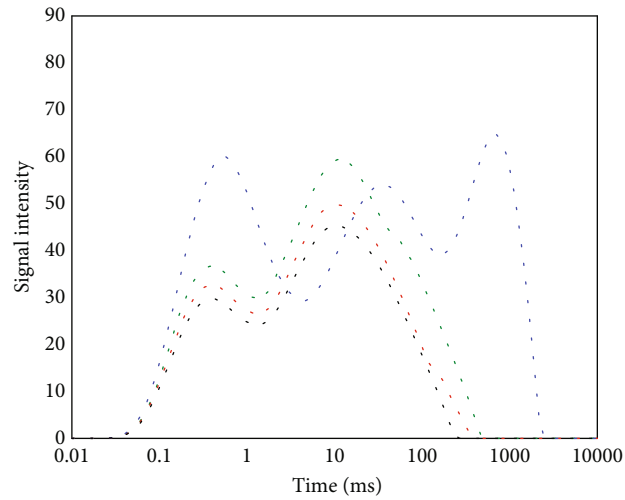

% (saturated water before filtration)
% (saturated oil before filtration)
% (saturated water after filtration)
% (saturated oil after filtration)

(c) Core slice A-3

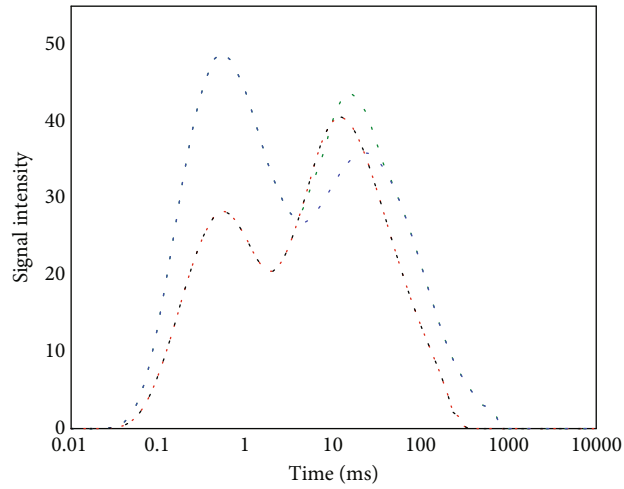

% (saturated water before filtration)
% (saturated oil before filtration)
% (saturated water after filtration)
% (saturated oil after filtration)

(d) Core slice A-4

Figure 11: Continued.

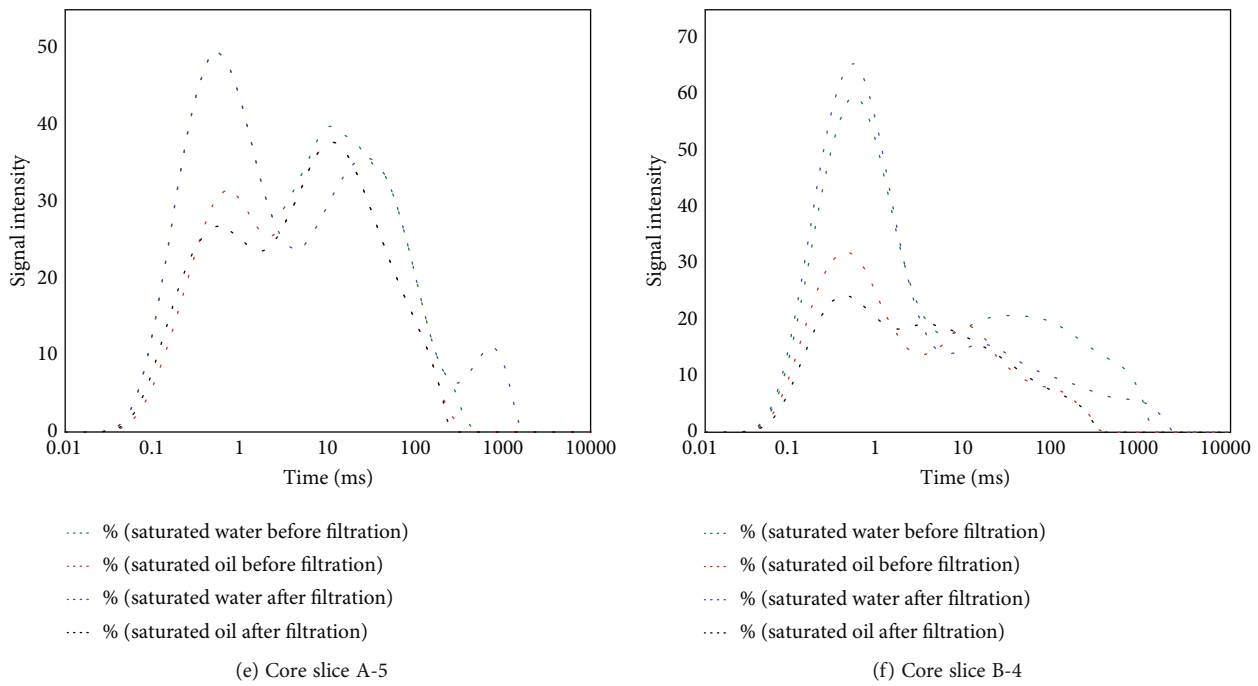

Figure 11: NMR spectra of different core slices.

Table 3: Mixed wettability test results of different core slices.

No.	Before fracturing fluid retention				After fracturing fluid retention			
	Hydrophilicity coefficient	Lipophilic coefficient	Mixed wettability	Wettability	Hydrophilicity coefficient	Lipophilic coefficient	Mixed wettability	Wettability
A-1	0.577	0.422	0.154	Weak hydrophilicity	0.572	0.427	0.145	Weak hydrophilicity
A-2	0.574	0.425	0.149	Weak hydrophilicity	0.608	0.391	0.217	Weak hydrophilicity
A-3	0.527	0.472	0.055	Neutral	0.649	0.350	0.299	Weak hydrophilicity
A-4	0.641	0.358	0.283	Weak hydrophilicity	0.655	0.344	0.311	Hydrophilicity
A-5	0.636	0.363	0.273	Weak hydrophilicity	0.639	0.360	0.278	Weak hydrophilicity
B-4	0.634	0.365	0.268	Weak hydrophilicity	0.715	0.284	0.430	Hydrophilicity

minerals, such as illite, with a large content in the reservoir in this area, is often filled by them, resulting in the narrowing or even disappearance of the pore throat, increasing the heterogeneity of the pore throat, and increasing the uncertainty and complexity of the fracturing fluid retention process. Therefore, there are a large number of clay minerals in the tight reservoir that affect the structure of the pore throat and lead to a significant increase in its microheterogeneity, making the pore throat thinner and poor connectivity, reducing the seepage channel and greatly reducing its permeability.

3.3. Influence of Retained Fracturing Fluids on Wettability. The wettability is evaluated according to the evaluation standard of wettability. When the mixed wettability index is greater than 0, it indicates that the hydrophilic part in the core is more than the lipophilic part, which generally shows the hydrophilic characteristics. The higher value will cause stronger hydrophilicity of the core. When the mixed wettability index is less than 0, it indicates that the lipophilic part of the core is more than the hydrophilic part, showing the characteristics of lipophilicity in general. The lower value indicates the stronger lipophilicity of the core. The measured T2 spectrum is shown in Figure 11.

The results of the mixed wettability of core slices are shown in Table 3. From the table, it shows that the average hydrophilic coefficient of core slices used in this experiment is 0.598. The average lipophilic coefficient is 0.402, and the average mixed wettability index is 0.196. The wettability is generally weak and hydrophilic. The average hydrophilicity coefficient, oil affinity coefficient, and mixed wettability

index of the core slice measured again after the retention of the fracturing fluids are 0.640, 0.360, and 0.280, respectively. It can be seen that the mixed wettability index of the core slice before and after the retention of the fracturing fluids increases slightly, but it is still in the range of weak hydrophilicity. Therefore, the retained fracturing fluids during the fracturing process have little impact on the reservoir wettability, and there is no wettability inversion.

4. Conclusions

Under laboratory experimental conditions, this paper studies the influence of retained fracturing fluids on reservoir physical properties by using core thin section and nuclear magnetic resonance technology, clarifies the distribution of retained fracturing fluids in the core, and reveals the influence rule of retained fracturing fluids on tight reservoir permeability and wettability.

(1) The retention of fracturing fluids and oil in micropores is studied using nuclear magnetic resonance technology and a stereoscopic microscope. The main retention space of retained fracturing fluids in tight reservoirs is a microporous interval. The residual oil after displacement by retained fracturing fluids mainly exists in the core in the form of dots or patches

(2) There will be more retained fracturing fluids in the tight core. The smaller permeability and porosity of the core will cause the more retained fracturing fluids. The permeability of different cores after fracturing fluid retention has decreased to varying degrees compared with that before fracturing fluid retention. In tight reservoirs, clay minerals will expand or migrate when encountering retained fracturing fluids, which will occupy the pore space, reducing the porosity and poor permeability

(3) Using the method of evaluating the overall mixed wettability of tight cores, combining the indoor core physical simulation with nuclear magnetic resonance technology, the wettability of core slices before and after the test is tested, and the retained fracturing fluids has no significant impact on the reservoir wettability

Data Availability

Data is available by contacting the corresponding author.

Conflicts of Interest

The authors declare that they have no conflicts of interest.

Acknowledgments

This study was supported by the National Natural Science Foundation of China (grant nos. 51874242 and 51934005).

References

[1] S. Longde, Z. Caineng, J. Ailin et al., "Development characteristics and orientation of tight oil and gas in China," *Petroleum Exploration and Development*, vol. 46, no. 6, pp. 1015–1026, 2019.

[2] B. Liu, Y. Yang, J. Li, Y. Chi, J. Li, and X. Fu, "Stress sensitivity of tight reservoirs and its effect on oil saturation: a case study of lower cretaceous tight clastic reservoirs in the Hailar Basin, Northeast China," *Journal of Petroleum Science and Engineering*, vol. 184, article 106484, 2020.

[3] Y. Xie, X. Liu, J. Wang, N. Wu, C. Hu, and Y. Wang, "Characteristics and main controlling factors of tight oil reservoirs in Chang 7 member of Yanchang formation in Ordos Basin, North Shaanxi," *Marine Geology & Quaternary Geology*, vol. 42, no. 3, pp. 149–159, 2022.

[4] D. Zhang, L. Zhang, T. A. Huiying, and Z. H. Yulong, "Fully coupled fluid-solid productivity numerical simulation of multistage fractured horizontal well in tight oil reservoirs," *Petroleum Exploration and Development*, vol. 49, no. 2, pp. 338–347, 2022.

[5] J. Wang, H. Q. Liu, G. B. Qian, and Y. C. Peng, "Mechanisms and capacity of high-pressure soaking after hydraulic fracturing in tight/shale oil reservoirs," *Petroleum Science*, vol. 18, no. 2, pp. 546–564, 2021.

[6] B. B. Williams, "Fluid loss from hydraulically induced fractures," *Journal of Petroleum Technology*, vol. 22, no. 7, pp. 882–888, 1970.

[7] C. H. Yew, M. J. Ma, and A. D. Hill, "A study of fluid leakoff in hydraulic fracture propagation," in *International Oil and Gas Conference and Exhibition in China*, Beijing, China, 2000.

[8] J. L. Rodgerson, "Impact of natural fractures in hydraulic fracturing of tight Gas Sands," in *SPE Permian Basin Oil and Gas Recovery Conference*, Midland, Texas, 2000.

[9] H. D. Outmans, "Mechanics of static and dynamic filtration in the borehole," *Society of Petroleum Engineers Journal*, vol. 3, no. 3, pp. 236–244, 1963.

[10] P. S. Vinod, M. L. Flindt, R. J. Card, and J. P. Mitchell, "Dynamic fluid-loss studies in low-permeability formations with natural fractures," in *SPE production operations Symposium*, Oklahoma City, Oklahoma, 1997.

[11] S. A. Mathias and M. Van Reeuwijk, "Hydraulic fracture propagation with 3-D leakoff," *Transport in Porous Media*, vol. 80, no. 3, pp. 499–518, 2009.

[12] B. Hou, Z. Cui, J.-H. Ding, F.-S. Zhang, L. Zhuang, and D. Elsworth, "Perforation optimization of layer-penetration fracturing for commingling gas production in coal measure strata," *Petroleum Science*, vol. 19, no. 4, pp. 1718–1734, 2022.

[13] Q. A. Da, C. J. Yao, X. Zhang, X. P. Wang, X. H. Qu, and G. L. Lei, "Investigation on microscopic invasion characteristics and retention mechanism of fracturing fluid in fractured porous media," *Petroleum Science*, vol. 19, no. 4, pp. 1745–1756, 2022.

[14] J. Lu, B. Hao, C. Li, W. Wang, Q. Wang, and W. Yang, "Permeability prediction of tight sandstone reservoirs based on flow unit classification," *Petroleum Science Bulletin*, vol. 3, pp. 369–379, 2021.

[15] S. J. Pirson, E. M. Boatman, and R. L. Nettle, "Prediction of relative permeability characteristics of intergranular reservoir rocks from electrical resistivity measurements," *Journal of Petroleum Technology*, vol. 16, no. 5, pp. 564–570, 1964.

[16] K. O. Akande, T. O. Owolabi, S. O. Olatunji, and A. AbdulRaheem, "A hybrid particle swarm optimization and support vector regression model for modelling permeability prediction of hydrocarbon reservoir," *Journal of Petroleum Science and Engineering*, vol. 150, no. 2, pp. 43–53, 2017.

[17] W. R. Purcell, "Capillary pressures - their measurement using mercury and the calculation of permeability therefrom," *Journal of Petroleum Technology*, vol. 1, no. 2, pp. 39–48, 1949.

[18] J. H. M. Thomeer, "Introduction of a pore geometrical factor defined by the capillary pressure curve," *Journal of Petroleum Technology*, vol. 12, no. 3, pp. 73–77, 1960.

[19] J. H. M. Thomeer, "Air permeability as a function of three pore-network parameters," *Journal of Petroleum Technology*, vol. 35, no. 4, pp. 809–814, 1983.

[20] S. J. Kolodzie, "Analysis of pore throat size and use of the Waxman-Smits equation to determine OOIP in Spindle field, Calorado," in *SPE Annual Technical Conference and Exhibition*, Dallas, Texas, 1980.

[21] M. R. Rezaee, A. Saeedi, and B. Clennell, "Tight gas sands permeability estimation from mercury injection capillary pressure and nuclear magnetic resonance data," *Journal of Petroleum Science and Engineering*, vol. 12, pp. 92–99, 2012.

[22] K. B. Min, J. Rutqvist, C. F. Tsang, and L. Jing, "Stress-dependent permeability of fractured rock masses: a numerical study," *International Journal of Rock Mechanics and Mining Sciences*, vol. 41, no. 7, pp. 1191–1210, 2004.

[23] B. Larsen, I. Grunnaleite, and A. Gudmundsson, "How fracture systems affect permeability development in shallow-water carbonate rocks: an example from the Gargano Peninsula, Italy," *Journal of Structural Geology*, vol. 32, no. 9, pp. 1212–1230, 2010.

[24] Z. Meng, S. L. Yang, Y. Cui et al., "Enhancement of the imbibition recovery by surfactants in tight oil reservoirs," *Petroleum Science*, vol. 15, no. 4, pp. 783–793, 2018.

[25] J. Wang, L. Z. Xiao, G. Z. Liao et al., "NMR characterizing mixed wettability under intermediate-wet condition," *Magnetic Resonance Imaging*, vol. 56, pp. 156–160, 2019.

[26] Y. Zhang, H. Ge, Y. Shen, L. Jia, and J. Wang, "Evaluating the potential for oil recovery by imbibition and time-delay effect in tight reservoirs during shut-in," *Journal of Petroleum Science and Engineering*, vol. 184, article 106557, 2020.

[27] J. J. Howard, "Quantitative estimates of porous media wettability from proton NMR measurements," *Magnetic Resonance Imaging*, vol. 16, no. 5-6, pp. 529–533, 1998.

[28] C. Straley, C. E. Morriss, W. E. Kenyon, and J. J. Howard, "NMR in partially saturated sandstones: laboratory insights into free fluid index, and comparison with borehole logs," *The Log Analyst*, vol. 36, pp. 40–56, 1995.

[29] M. Fleury and F. Deflandre, "Quantitative evaluation of porous media wettability using NMR relaxometry," *Magnetic Resonance Imaging*, vol. 21, no. 3-4, pp. 385–387, 2003.

[30] H. Guan, D. Brougham, K. S. Sorbie, and K. J. Packer, "Wettability effects in a sandstone reservoir and outcrop cores from NMR relaxation time distributions," *Journal of Petroleum Science and Engineering*, vol. 34, no. 1-4, pp. 35–54, 2002.

[31] S. H. Al-Mahrooqi, C. A. Grattoni, A. H. Muggeridge, R. W. Zimmerman, and X. D. Jing, "Pore-scale modelling of NMR relaxation for the characterization of wettability," *Journal of Petroleum Science and Engineering*, vol. 52, no. 1-4, pp. 172–186, 2006.

[32] E. B. Johannesen, H. Riskedal, L. Tipura, J. J. Howard, and A. Graue, "Wettability characterization by NMR T2 measurements in Edwards limestone rock," in *International Symposium of the Society of Core Analysts*, pp. 10–13, Calgary, Canada, 2007.

[33] J. Chen, G. J. Hirasaki, and M. Flaum, "NMR wettability indices: effect of OBM on wettability and NMR responses," *Journal of Petroleum Science and Engineering*, vol. 52, no. 1-4, pp. 161–171, 2006.

[34] C. C. Minh, S. Crary, P. M. Singer et al., "Determination of wettability from magnetic resonance relaxation and diffusion measurements on fresh-state cores," in *SPWLA 56th Annual Logging Symposium*, Long Beach, California, USA, 2015.

[35] A. Rabiei, M. Sharifinik, A. Niazi, A. Hashemi, and S. Ayatollahi, "Core flooding tests to investigate the effects of IFT reduction and wettability alteration on oil recovery during MEOR process in an Iranian oil reservoir," *Applied Microbiology and Biotechnology*, vol. 97, no. 13, pp. 5979–5991, 2013.

[36] D. H. Pratten and R. G. Craig, "Wettability of a hydrophilic addition silicone impression material," *Journal of Prosthetic Dentistry*, vol. 61, no. 2, pp. 197–202, 1989.

[37] C. Gachot, M. Hans, R. Catrin, U. Schmid, and F. Mücklich, "Tuned wettability of material surfaces for tribological applications in miniaturized systems by laser interference metallurgy," in *Smart Sensors, Actuators, and MEMS IV (Vol. 7362, pp. 242-250)*, Dresden, Germany, 2009.

[38] Y. Zhang, Y. Zou, Y. Zhang et al., "Experimental study on characteristics and mechanisms of matrix pressure transmission near the fracture surface during post-fracturing shut-in in tight oil reservoirs," *Journal of Petroleum Science and Engineering*, vol. 219, article 111133, 2022.

[39] G. Chunyuan, Q. I. Rongsheng, D. I. Qinfeng, F. Jiang, and C. H. Huijuan, "Simulation and visualization experiment of manganese ion diffusion and damage to gel in a porous media-gel system," *Petroleum Exploration and Development*, vol. 46, no. 2, pp. 354–360, 2019.

[40] M. Meng, L. Li, B. Yuan et al., "Influence of overburden pressure on imbibition behavior in tight sandstones using nuclear magnetic resonance technique," *Journal of Energy Resources Technology*, vol. 145, no. 7, article 073302, 2023.

[41] Y. L. Su, J. L. Xu, W. D. Wang, H. Wang, and S. Y. Zhan, "Relative permeability estimation of oil–water two-phase flow in shale reservoir," *Petroleum Science*, vol. 19, no. 3, pp. 1153–1164, 2022.